



# A model for predicting tensile modulus of polymer nanocomposites reinforced with cellulose nanocrystals

Ali Mohammadpour-Haratbar · Ziba Bouchani ·  
Yasser Zare · Nima Gharib · Kyong Yop Rhee

Received: 27 February 2023 / Accepted: 13 August 2023 / Published online: 21 August 2023  
© The Author(s), under exclusive licence to Springer Nature B.V. 2023

**Abstract** In this paper, the Young's modulus of composites containing cellulose nanocrystals (CNCs) is predicted using a simple model. The significance of interphase and CNC dimensions on the nanocomposite modulus was analyzed using the developed model, which was validated using experimental data from a variety of samples. The modulus predictions were in accordance with the measured data, and CNC volume fraction of 0.02 increased the modulus of the system by 65%. Moreover, a nanocomposite that included thinner and longer CNCs had a greater modulus, and the nanocomposite modulus increased by 29.9% when the interphase thickness was 30 nm. Additionally, the

modulus of the nanocomposite increased by 35.3% at an interphase modulus of 10 GPa, whereas the modulus of the system increased by 38.4% at an interphase modulus of 60 GPa. Therefore, a thicker and stiffer interphase caused a higher modulus for nanocomposites. Generally, the interphase features and CNC length directly controlled the stiffness of the system, whereas the CNC diameter had an opposite effect.

**Keywords** Polymer nanocomposites · Cellulose nanocrystals · Nanofiller · Young's Modulus · Model · Interphase region

A. Mohammadpour-Haratbar · Y. Zare (✉)  
Department of Interdisciplinary Technologies,  
Biomaterials and Tissue Engineering Research Group,  
Breast Cancer Research Center, Motamed Cancer Institute,  
ACECR, Tehran, Iran  
e-mail: y.zare@aut.ac.ir

Z. Bouchani  
Control and Intelligent Processing Center of Excellence,  
School of Electrical and Computer Engineering,  
University of Tehran, Tehran 14395/515, Iran

N. Gharib  
College of Engineering and Technology, American  
University of the Middle East, Egaila 54200, Kuwait

K. Y. Rhee (✉)  
Department of Mechanical Engineering (BK21 four),  
College of Engineering, Kyung Hee University, Yongin,  
Republic of Korea  
e-mail: rheekey@khu.ac.kr

## Introduction

The synergistic interaction between a polymer matrix and nanofillers produces extraordinary properties in polymer nanocomposites (PNCs), attracting the attention of researchers. Moreover, nanofillers in polymer matrices can improve the electrical and mechanical properties of the final nanocomposite by acting as conducting and reinforcing agents (Aboueimehrizi et al. 2022; Alam et al. 2016; Hajduk et al. 2021; Hatami et al. 2022; Jung and Sodano 2022; Saleh et al. 2022). These improved properties have resulted in the wide acceptance of PNCs in a variety of fields, including electronics, electromagnetic interference (EMI) shielding, biosensors, drug delivery systems, and biomedical applications. (Bhat et al. 2021; Han et al. 2022;

Mohammadpour-Haratbar et al. 2022b; Rivera-Briso et al. 2020).

Recently, the use of cellulose nanocrystals (CNCs) as innovative nanofiller for PNCs has attracted a significant amount of attention. CNCs are composed of highly crystalline regions (approximately 54–88%), short rod-like shapes, diameters of 2–20 nm, and lengths of 100–500 nm (Bai et al. 2022; Ding et al. 2022; Kandhola et al. 2022; Zhou et al. 2022). Furthermore, they achieved a Young's modulus of 140 GPa and a strength of approximately 7.5 GPa (Wang et al. 2015). Accordingly, CNCs exhibit a range of exceptional properties, such as high aspect ratios, large surface areas, and outstanding mechanical performance, rendering them ideal for adding to polymer matrices (Jahan et al. 2018). CNCs are non-toxic and offer interesting surface chemistry, which make them suitable for biomedical applications such as electrochemical biosensors and drug delivery systems (Liu et al. 2019). In other words, CNCs are considered as bio-based nanostructures with unique properties that can be used as nanomaterials within PNCs for the detection and treatment of a variety of cancers, particularly breast cancer (Pinto et al. 2021). Therefore, researchers in the field of breast cancer diagnosis and treatment may benefit from the use of an applicable model for examining the mechanical properties of CNC-based PNCs.

Researchers have developed a number of models for estimating the Young's modulus of conventional composites. Here, polymer matrix properties (such as matrix modulus) and filler properties such as filler size and volume fraction are considered in the calculations. However, the interface/interphase between the filler and polymer matrix is not considered (Ku et al. 2011; Wan and Chen 2012; Xie et al. 2004). It is important to consider how the interface affects the mechanical properties of PNCs because nanoparticles have a large surface area and strong interfacial interactions with the polymer matrix, which can result in the formation of an interphase around the nanoparticles (Baek et al. 2021; Kirmani et al. 2022; Power et al. 2021; Razavi et al. 2017; Zare 2016; Zare and Rhee 2017a, 2020, 2022b, c). The mechanical

properties of PNCs are mainly influenced by the interphase properties, including thickness and stiffness (Yang et al. 2020; Zare and Rhee 2018, 2022d, 2023; Zare et al. 2022a). Using these models, the mechanical properties of the interphase can be estimated based on experimental results.

Takayanagi et al. (1964) suggested an equation for calculating the modulus of composites based on the matrix modulus and the filler features (amount and modulus). However, since the interphase region is ignored, this model cannot be used to calculate the modulus of a nanocomposite. In this paper, Takayanagi equation is extended for the modulus of CNC-containing systems by adding interphase aspects (modulus and thickness) and CNC size. Several factors are considered in the developed model, including real filler concentration, CNC size, and interphase modulus. Due to the inclusion of both CNCs and interphase regions in this model, it is suitable for estimating the modulus of nanocomposites. Furthermore, by the experimental moduli of several samples and an explanation of the effects of all factors on the modulus of PNCs, the accuracy of the proposed model is evaluated.

## Theoretical model

According to the Takayanagi model, the modulus of PNCs is correlated with the polymer matrix and particles properties as follows:

$$E = E_m \left[ (1 - A) + \frac{B}{(1 - A) + B \frac{E_f}{E_m}} \right]^{-1} \quad (1)$$

$$A = B = \sqrt{\phi_f} \quad (2)$$

The Young's moduli of polymer matrixes and fillers are denoted by “ $E_m$ ” and “ $E_f$ ,” respectively, while the filler volume fraction is represented by “ $\phi_f$ .” However, because the interphase zone is ignored in this model, estimation of the modulus of every PNC is not possible. Assuming that the interphase regions

and CNC aspect ratio are operative factors, this equation can approximate the modulus of CNC-based nanocomposites. The Takayanagi model is updated with interphase properties and CNC size as follows:

$$E = E_m \left[ (1 - A) + \frac{B}{H} + \frac{A}{a} + \frac{B}{(1 - A) + B \frac{E_f}{E_m}} \right]^{-1} \tag{3}$$

$$A = \sqrt{\phi_{eff}} \tag{4}$$

$$B = \sqrt{\phi_f} \tag{5}$$

$$H = \frac{E_i}{E_m} \tag{6}$$

“a” denotes the aspect ratio of CNCs ( $a = \frac{l}{d}$ ), where “l” and “d” represent the length and diameter of the CNCs, respectively. Term “ $\phi_{eff}$ ” refers to the filler concentration and “ $E_i$ ” denotes the interphase modulus around the CNCs. An appropriate consideration of the CNCs and interphase regions in PNCs is present in this model. As a result, all parameters included in the proposed model are expressive and easily understood, affirming its rationality.

The interphase volume portion in a sample containing rod-like nanofillers can be obtained (Mohammadpour-Haratbar et al. 2022a) using the following:

$$\phi_i = \phi_f \left[ \left( 1 + 2 \frac{t}{d} \right)^2 - 1 \right] \tag{7}$$

where “t” is the thickness of the interphase.

It is important to consider the volume fractions of CNCs and interphase when calculating the effective CNC concentration since both of these terms control the reinforcing of nanocomposites. Therefore, the value of  $\phi_{eff}$  can be calculated using the following:

$$\phi_{eff} = \phi_f + \phi_i = \phi_f \left( 1 + 2 \frac{t}{d} \right)^2 \tag{8}$$

which concerns the main parameters, comprising CNC content, CNC diameter, and interphase thickness.

In Eq. (4), the value of  $\phi_{eff}$  can be exchanged with the value in Eq. (8) as follows:

$$A = \sqrt{\phi_f \left( 1 + 2 \frac{t}{d} \right)^2} \tag{9}$$

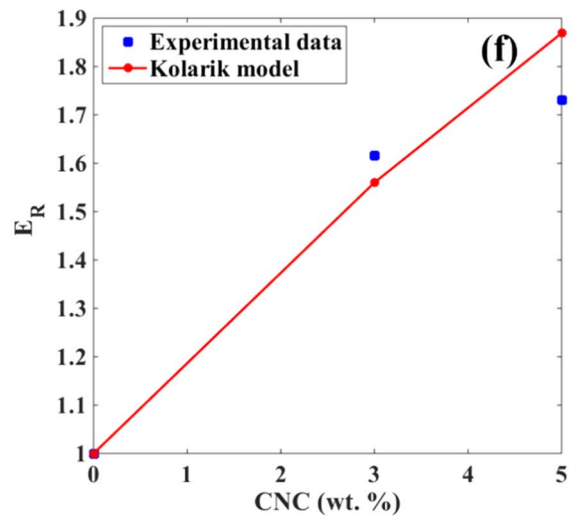
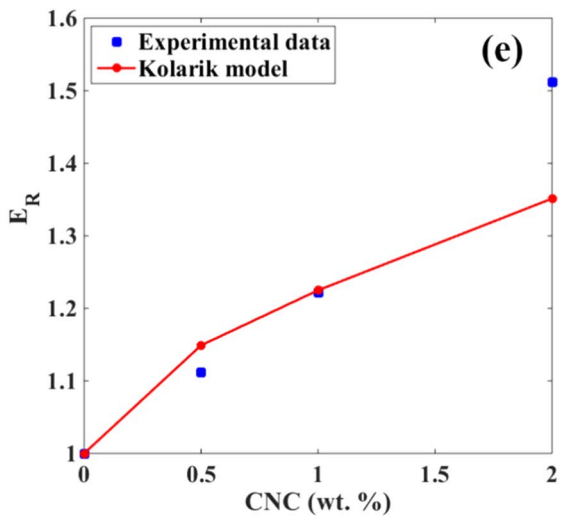
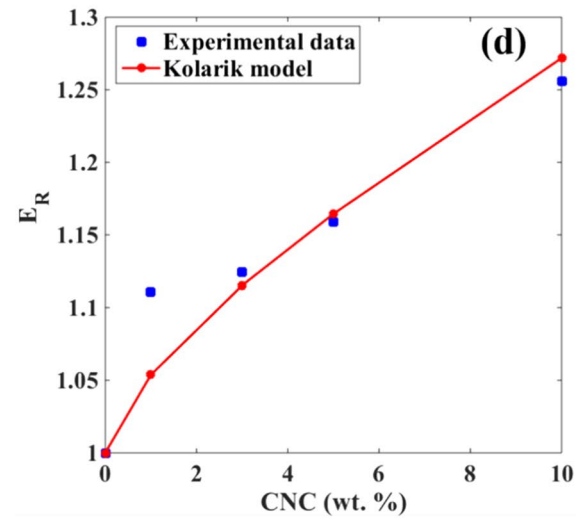
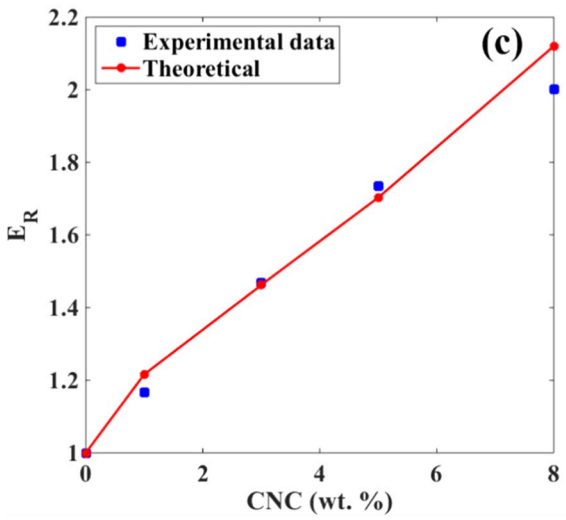
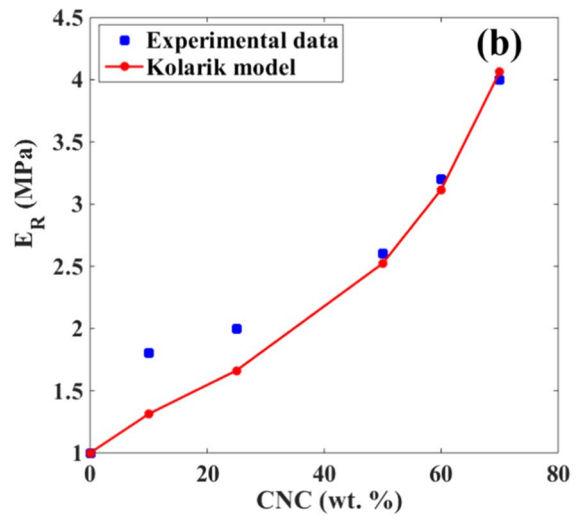
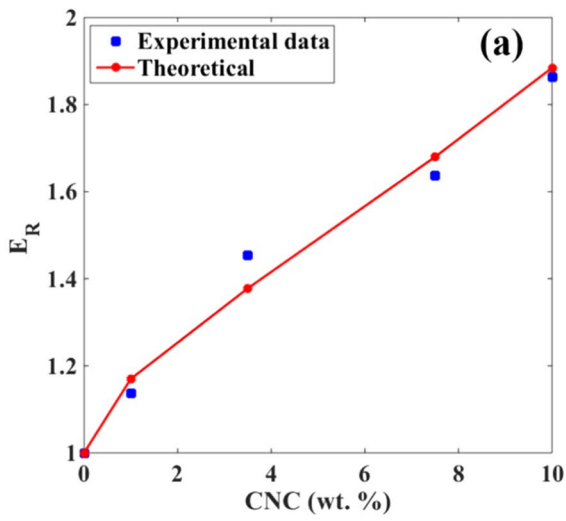
supposing the characters of CNC volume fraction, interphase thickness, and CNC length in “A”.

By substituting Eqs. (4)–(9) into Eq. (3), the relative modulus ( $E_R = E/E_m$ ) can be stated as follows:

$$E_R = \left[ \left( 1 - \sqrt{\phi_f \left( 1 + 2 \frac{t}{d} \right)^2} \right) + \frac{E_m \sqrt{\phi_f}}{E_i} + \frac{\sqrt{\phi_f \left( 1 + 2 \frac{t}{d} \right)^2}}{a} + \frac{\sqrt{\phi_f}}{\left( 1 - \sqrt{\phi_f \left( 1 + 2 \frac{t}{d} \right)^2} \right) + \frac{\sqrt{\phi_f} E_f}{E_m}} \right]^{-1} \tag{10}$$

**Table 1** CNC-based samples from published papers and their details from references and proposed model

Samples (Ref.)	$E_m$ (GPa)	d (nm)	l ( $\mu$ m)	t (nm)	$E_i$ (GPa)
PEO/CNC Reid et al. (2018)	0.22	10	0.5	4	15
CMC/CNC Wang et al. (2015)	2.5	9	0.165	1.15	13.5
k-CA/CNC Kassab et al. (2019)	1.5	5	0.275	4	26
PP/CNC Gwon et al. (2018]	5.18	10	0.154	1.3	32
PES/CNC Bai et al. (2017)	0.045	5	0.2	2.6	18
epoxy/CNC Qiu et al. (2021)	0.0065	12.5	0.175	10.5	25



◀**Fig. 1** Tested and foreseen records by the proposed model for **a** PEO/CNC (Reid et al. 2018), **b** CMC/CNC (Wang et al. 2015), **c** k-CA/CNC (Kassab et al. 2019), **d** PP/CNC (Gwon et al. 2018), **e** PES/CNC (Bai et al. 2017), and **f** epoxy/CNC (Qiu et al. 2021) samples

which associates the  $E_R$  of the CNC-based nanocomposite to the CNC volume fraction, CNC size (diameter and length), interphase thickness and modulus, and CNC modulus.

## Results and discussions

### Connection between tested data and theoretical predictions

The approximations from the proposed model were used to determine the tentative  $E_R$  values for various examples. Data from real samples containing a polymer matrix and CNCs of different types can prove the accuracy of proposed model. Table 1 lists samples and their properties from related papers. More details about these samples can be found in the original references, including the fabrication processes. The “ $E_R$ ” is calculated at abundant CNC contents stated in the references using polymer matrix modulus and CNC size by Eq. (10). According to the reports, CNCs have a modulus of 140 GPa (Shin et al. 2022; Tang et al. 2017). The  $E_R$  results from the experiment and the proposed model for the samples are displayed in Fig. 1a–f, which indicated good agreement between the actual and theoretical values and proved that the simple model was accurate when estimating the moduli of CNC-based samples. It is evident that the tentative modulus data for various kinds of samples validate the proposed model.

The interphase thickness ( $t$ ) and interphase modulus ( $E_i$ ) of the examples were calculated using the proposed model, as shown in Table 1. The epoxy/CNC sample exhibited the largest interphase thickness ( $t$ ) of 10.5 nm, while the CMC/CNC sample exhibited the thinnest interphase region of 1.15 nm. Given that the values for interphase thickness vary at the nanoscale, all of these results were reasonable. In addition, the PP/CNC nanocomposite had a maximum interphase modulus ( $E_i$ ) of 32 GPa, whereas the CMC/CNC nanocomposite had a minimum interphase modulus of 13.5 GPa. In other words, the PP/

CNC nanocomposite contained the strongest interphase region, while CMC/CNC nanocomposite had the weakest one.

### Relationship between predicted moduli and parameters

Various extents of each parameter were considered in the proposed model to rationalize the role of each parameter in the  $E_R$  value. Using average ranges of  $l=0.5$  mm,  $\phi_f = 0.01$ ,  $E_m = 2$  GPa,  $d=10$  nm,  $t=10$  nm, and  $E_i = 30$  GPa, the patterns exhibited the influence of one parameter on the  $E_R$ . Plots depict the relationship between  $E_R$  and a specified parameter that facilitates optimization.

Figure 2 illustrates the impact of CNC volume fraction on  $E_R$  values when applied to the proposed model. Here, CNC volume fraction of 0 caused  $E_R$  of 1 (modulus of the polymer matrix), while CNC volume fraction of 0.02 created  $E_R$  of 1.65. The plot indicates that the CNC volume fraction directly influenced the PNC modulus. Moreover, the higher the CNC content, the greater the modulus. Consequently, CNC concentration played a major role in adjusting the modulus of the PNCs, since it mostly affected the  $E_R$  from 1 to 1.65.

Because CNCs are harder than the polymer, a higher proportion of CNCs yields a stronger PNC. Moreover, a high CNC content increases the effectiveness of the reinforcement phase, which increases the stiffness. In contrast, PNCs with a low CNC content have a decreased modulus due to the weakened reinforcement. Because CNCs are tougher than the polymer matrix and interphase region, it determines the degree of reinforcement in nanocomposites. The filler concentration term is included in all conventional and novel models for nanocomposites because this plays a crucial role in the reinforcement of materials (Jamali et al. 2022; Mohammadpour-Haratbar et al. 2022a). Therefore, the proposed model satisfactorily correlated the modulus of PNCs with the CNC volume fraction.

Based on several ranges of CNC diameter, Fig. 3 illustrates the estimations from the proposed model. When  $d=5$  nm, the  $E_R$  had a maximum value of 1.9, while at  $d=20$  nm, it had a minimum value of 1.2. Therefore, the CNC diameter adversely affected the PNC modulus. Although denser CNCs produced a poorer PNC, narrower CNCs produced a higher

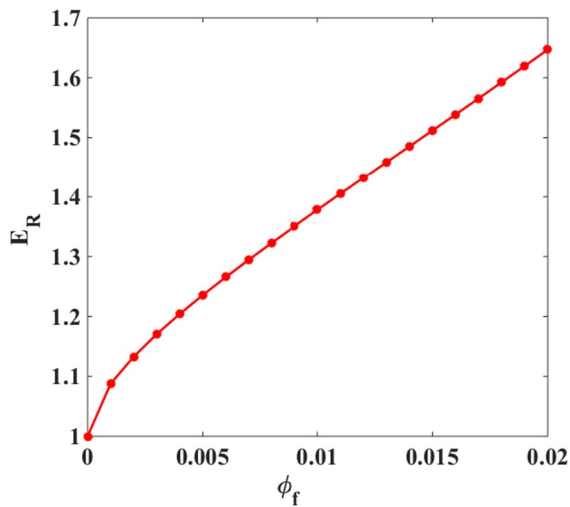


**Fig. 2** Effect of CNC volume fraction on  $E_R$  using the proposed model

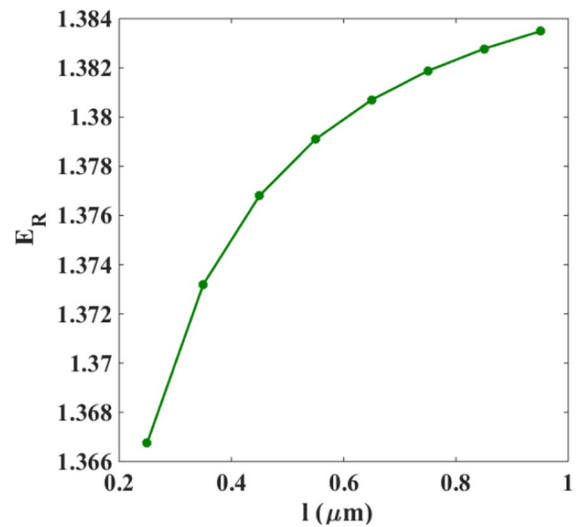


**Fig. 4** Influence of CNC length on  $E_R$

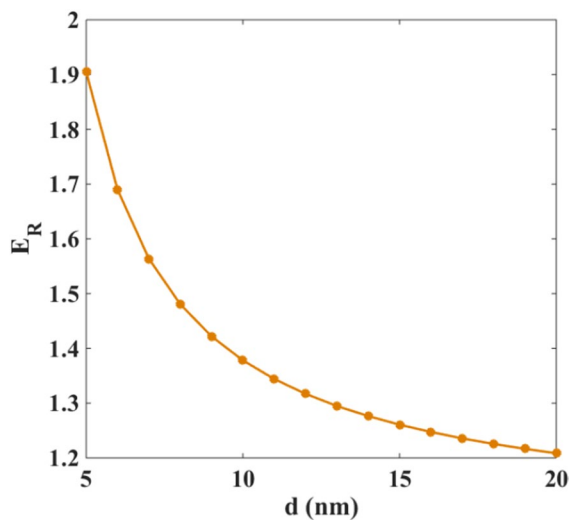


**Fig. 3** Outputs of the proposed model at many CNC diameter ranges

nanocomposite modulus. Accordingly, researchers should attempt to reduce the CNC diameter to develop nanocomposites with an improved modulus.

According to Eq. (7), narrow CNCs expand the interphase region in nanocomposites. Furthermore, according to Eq. (8), a small CNC diameter results in a highly effective volume fraction of the filler. Thus, narrow CNCs increase the effectiveness of fillers in the nanocomposite. Thin CNCs are

beneficial to the reinforcement of nanocomposites due to their positive influence on interphase concentration and effective filler volume fraction. In contrast, thick CNCs reduce the interphase content and effective filler content. Due to the minimization of the interphase region, thick CNCs significantly reduce the modulus of PNC. In addition, many models have revealed that the filler diameter adversely affects the mechanical performance of PNCs (Jamali et al. 2022; Zare and Rhee 2022a; Zare et al. 2022b). Therefore, the proposed model accurately related the  $E_R$  to CNC diameter.

Figure 4 displays the effect of CNC length on the  $E_R$  values calculated by the proposed model. Here, the  $E_R$  value for the CNC length of 0.25  $\mu\text{m}$  was 1.36, while  $E_R$  increased to 1.38 at the CNC length of 1  $\mu\text{m}$ . Thus, CNC length directly affected the modulus of the PNCs, and longer CNCs improved the modulus. Thus, nanocomposites with a higher modulus could be developed by increasing the CNC length.

Long CNCs can stiffen nanocomposites since they increase the surface contact between the polymer matrix and the CNCs. Thus, longer CNCs have more polymer phases, which cause the nanocomposite to have an increased modulus. Conversely, short CNCs cover fewer polymer chains, resulting in low stiffness. As a result, large CNCs can interact with many polymer chains, while shorter CNCs are incapable of covering the polymer matrix adequately.

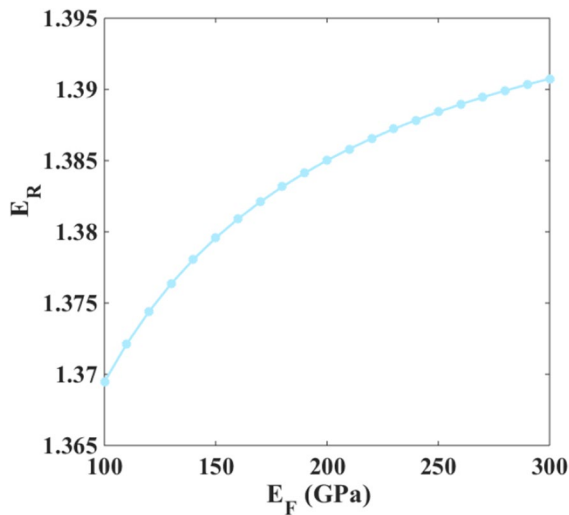


**Fig. 5** Correlation between  $E_R$  and CNC modulus based on the proposed model

Generally, the length of the CNCs affects the aspect ratio, adjusting the modulus of PNCs. Therefore, assuming Eq. (10), CNC length directly manipulates the modulus of PNCs.

Figure 5 illustrates how the CNC modulus affected  $E_R$  according to the proposed model.  $E_R = 1.369$  was obtained at the CNC modulus of 100 GPa, compared to 1.39 at the CNC modulus of 300 GPa. Consequently, the CNC modulus directly affected the modulus of the PNCs. Stronger CNCs are

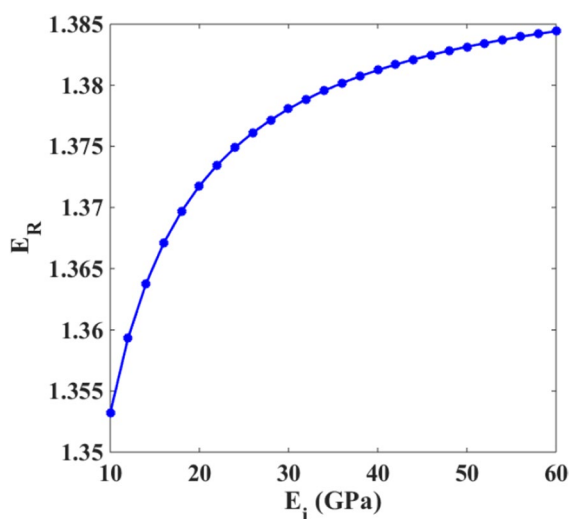


**Fig. 6** Effect of interphase modulus on  $E_R$ .

necessary for a tougher nanocomposite. In general, nanocomposites can be reinforced with robust CNCs, although they cannot be stiffened with poor CNCs.

The nanocomposites were strengthened significantly by tougher CNCs because stiffer phases were established in the samples. Alternatively, poor CNCs resulted in poor reinforcing because nanoparticle reinforcing is ineffective. As a result of the excellent modulus of nanoparticles, the system received a large amount of reinforcement. Hence, nanofillers that are exceptionally rigid can act as reinforcements for a polymer media that is in a poor condition. Therefore,  $E_R$  can be directly correlated with the CNC modulus.

Based on the proposed model, Fig. 6 illustrates the results of  $E_R$  at several interphase moduli. Here,  $E_R$  was 1.353 at  $E_i = 10$  GPa, which increased to 1.384 at  $E_i = 60$  GPa. Consequently, the uppermost interphase modulus created the stiffest system, based on the direct relationship between the interphase modulus and the sample modulus. At small levels of interphase modulus, the modulus of the examples increased significantly, although the modulus was negligibly affected at upper levels of more than 50 GPa. Consequently, interphase moduli that were too high did not contribute significantly to the nanocomposite modulus.

It is reasonable to assume a direct relationship between the moduli of a PNC and the interphase since a system modulus correlates with the moduli of

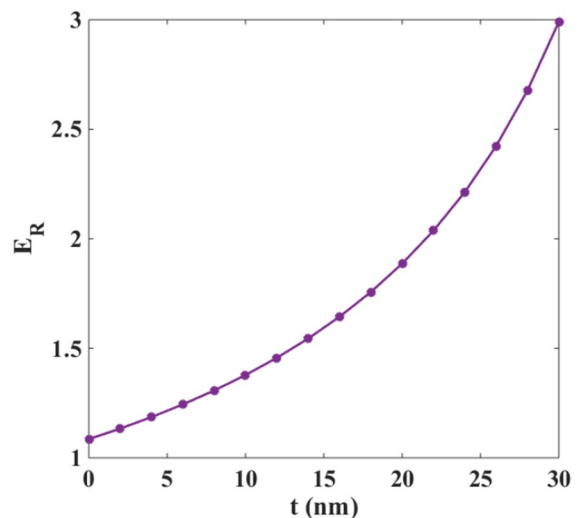


**Fig. 7** Relationship between  $E_R$  and interphase thickness based on the proposed model



the components. The presence of a sturdier interphase zone indicates that a system has a stronger component, which increases its modulus. Moreover, a more solid interphase enhances the stiffness by facilitating stress transport, whereas a weaker interphase cannot support the load, weakening the sample (Kundalwal and Kumar 2016; Zappalorto et al. 2011). Accordingly, the modulus of the interphase determines the reinforcement of a system, meaning the system modulus directly correlates with the interphase modulus, proving the proposed model is valid.

According to the proposed model, Fig. 7 illustrates the relationship between  $E_R$  and interphase thickness. When the interphase thickness was absent,  $E_R$  was 1.085, whereas this increased to 2.99 at  $t=30$  nm. Thus, the interphase thickness directly affected the modulus of system, and the densest interphase region achieved the maximum modulus. This confirmation suggested that a deeper interphase would be required to achieve a higher modulus.

A deeper interphase area reveals a tougher interfacial attachment between the matrix and the nanoparticles (Lu et al. 2021; Zare and Rhee 2017b). As a result, a large interphase area provides better reinforcement, since a robust interface can stand against the significant degree of stress. In contrast, a thinner interphase results in a poorer interface, which reduces the stress transfer. Accordingly, a thick interphase intensifies the reinforcement, since an interphase is more solid than the medium. In contrast, a thin interphase reduces reinforcement, since it cannot create a strong section for strengthening. Hence, the presented novel model provides a reasonable link between the system modulus and interphase depth.

## Conclusions

The accuracy of Takayanagi model for determining the modulus of CNC-based nanocomposites was improved with regard to the interphase aspects and the size of CNCs. For many systems, there was an excellent agreement between the experimental and theoretical data. CNC volume fraction of 0.02 caused the  $E_R$  of 1.65, indicating that CNC concentration directly determined the stiffness. Moreover, the CNC length of 0.25  $\mu\text{m}$  yielded the  $E_R$  of 1.36, which increased to 1.38 at the CNC length of 1  $\mu\text{m}$ .

Therefore, longer CNCs are desirable to increase stiffness. The  $E_R$  improved to 1.9 with  $d=5$  nm, although it reduced to 1.2 with  $d=20$  nm. As a result, narrower CNCs result in a stiffer nanocomposite. The  $E_R$  value was 1.085 without an interphase region, which improved to 2.99 at  $t=30$  nm. Hence, a deeper interphase is also required to increase the stiffness. Moreover,  $E_R$  value of 1.353 was produced at  $E_i = 10$  GPa, compared to 1.384 at  $E_i = 60$  GPa. Therefore, the toughest nanocomposite is achieved by the sturdiest interphase. Some parameters including interphase thickness, CNC diameter, and CNC volume fraction usually affected the modulus of samples, while very high levels of interphase modulus, CNC modulus, and CNC length had less influence on the stiffness.

**Acknowledgments** This work was supported by the Basic Science Research Program through the National Research Foundation of Korea (NRF) funded by the Ministry of Education, Science and Technology (2022R1A2C1004437).

**Author contributions** AMH and YZ wrote the main manuscript text. ZB, NG and KYR revised the paper. All authors reviewed the manuscript.

**Funding** The authors have not disclosed any funding.

**Data availability** The data that support the findings of this study are available on request from corresponding author.

## Declarations

**Conflict of interest** The authors declare no competing interests.

**Consent for publication** All authors agreed to the publication in the submitted form.

## References

- Aboueimehrizi E, Makaremy MA, Bazrpash S, Noormohammadi F, Darestani YR, Nourany M (2022) Synthesis of high-modulus thermoset PUs of PCL-PTMG/CNW biomaterials with different soft domain architecture and composition for high shape memory performance. *Cellulose* 29:8651–8674
- Alam A, Meng Q, Shi G, Arabi S, Ma J, Zhao N, Kuan H-C (2016) Electrically conductive, mechanically robust, pH-sensitive graphene/polymer composite hydrogels. *Compos Sci Technol* 127:119–126
- Baek K, Shin H, Cho M (2021) Multiscale modeling of mechanical behaviors of Nano-SiC/epoxy nanocomposites with modified interphase model: effect of nanoparticle clustering. *Compos Sci Technol* 203:108572



- Bai L, Bossa N, Qu F, Winglee J, Li G, Sun K, Liang H, Wiesner MR (2017) Comparison of hydrophilicity and mechanical properties of nanocomposite membranes with cellulose nanocrystals and carbon nanotubes. *Environ Sci Technol* 51:253–262
- Bai H, Li Y, Zhang S, Ma P, Dong W (2022) Photo-crosslinkable poly (vinyl alcohol)/nanocrystalline cellulose composites with controllable performance and exceptional water vapor barrier property for packaging application. *Cellulose* 29:7721–7734
- Bhat A, Budholiya S, Raj SA, Sultan MTH, Hui D, Shah AUM, Safri SNA (2021) Review on nanocomposites based on aerospace applications. *Nanotechnol Rev* 10:237–253
- Ding C, Yue C, Su J, Wang H, Yang N, Cheng B (2022) Effects of oxidized cellulose nanocrystals on the structure and mechanical properties of regenerated collagen fibers. *Cellulose* 29:7677–7690
- Gwon J-G, Cho H-J, Lee D, Choi D-H, Lee S, Wu Q, Lee S-Y (2018) Physicochemical and mechanical properties of polypropylene-cellulose nanocrystal nanocomposites: effects of manufacturing process and chemical grafting. *BioResources* 13:1619–1636
- Hajduk B, Bednarski H, Jarka P, Janeczek H, Godzierz M, Tański T (2021) Thermal and optical properties of PMMA films reinforced with Nb<sub>2</sub>O<sub>5</sub> nanoparticles. *Sci Rep* 11:22531
- Han L, Li K, Fu Y, Yin X, Jiao Y, Song Q (2022) Multifunctional electromagnetic interference shielding 3D reduced graphene oxide/vertical edge-rich graphene/epoxy nanocomposites with remarkable thermal management performance. *Compos Sci Technol* 222:109407
- Hatami M, Rahnama N, Karimi-Maleh H, Djafarzadeh N, Qandalee M, Setva R, Karimi F, Durán-Valle CJ, López-Coca IM, Sharifi A (2022) Use of phosphorylated chitosan/alumina nanoadditives for polymer performance improvement. *Cellulose* 29:6677–6696
- Jahan Z, Niazi MBK, Gregersen ØW (2018) Mechanical, thermal and swelling properties of cellulose nanocrystals/PVA nanocomposites membranes. *J Ind Eng Chem* 57:113–124
- Jamali S, Zare Y, Rhee KY (2022) Modeling of mechanical behaviors and interphase properties of polymer/nano-diamond composites for biomedical products. *J Mat Res Technol* 19:2750–2758
- Jung J, Sodano HA (2022) Cellulose nanocrystal functionalized aramid nanofiber reinforced rubber compounds for tire tread application. *Cellulose* 29:7735–7749
- Kandhola G, Djiroleu A, Rajan K, Batta-Mpouma J, Labbé N, Sakon J, Babst BA, Ghosh A, Carrier DJ, Kim J-W (2022) Impact of species-based wood feedstock variability on physicochemical properties of cellulose nanocrystals. *Cellulose* 29:8213–8228
- Kassab Z, Aziz F, Hannache H, Youcef HB, El Achaby M (2019) Improved mechanical properties of k-carrageenan-based nanocomposite films reinforced with cellulose nanocrystals. *Int J Biol Macromol* 123:1248–1256
- Kirmani MH, Jony B, Gupta K, Kondekar N, Ramachandran J, Arias-Monje PJ, Kumar S (2022) Using a carbon fiber sizing to tailor the interface-interphase of a carbon nanotube-polymer system. *Compos B Eng* 247:110284
- Ku H, Wang H, Pattarachaiyakop N, Trada M (2011) A review on the tensile properties of natural fiber reinforced polymer composites. *Compos B Eng* 42:856–873
- Kundalwal SI, Kumar S (2016) Multiscale modeling of stress transfer in continuous microscale fiber reinforced composites with nano-engineered interphase. *Mech Mater* 102:117–131
- Liu S, Chen Y, Liu C, Gan L, Ma X, Huang J (2019) Polydopamine-coated cellulose nanocrystals as an active ingredient in poly (vinyl alcohol) films towards intensifying packaging application potential. *Cellulose* 26:9599–9612
- Lu X, Detrez F, Yvonne J, Bai J (2021) Identification of elastic properties of interphase and interface in graphene-polymer nanocomposites by atomistic simulations. *Compos Sci Technol* 213:108943
- Mohammadpour-Haratbar A, Zare Y, Rhee KY (2022) Development of a theoretical model for estimating the electrical conductivity of a polymeric system reinforced with silver nanowires applicable for the biosensing of breast cancer cells. *J Mater Res Technol* 18:4894–4902
- Mohammadpour-Haratbar A, Zare Y, Rhee KY (2022) Electrochemical biosensors based on polymer nanocomposites for detecting breast cancer: recent progress and future prospects. *Adv Colloid Interface Sci* 309:102795
- Pinto RJ, Lameirinhas NS, Guedes G, Rodrigues da Silva GH, Oskoei P, Spirk S, Oliveira H, Duarte IF, Vilela C, Freire CS (2021) Cellulose nanocrystals/chitosan-based nanosystems: synthesis, characterization, and cellular uptake on breast cancer cells. *Nanomaterials* 11:2057
- Power AJ, Remediakis IN, Harmandaris V (2021) Interface and interphase in polymer nanocomposites with bare and core-shell gold nanoparticles. *Polymers* 13:541
- Qiu K, Tannenbaum R, Jacob KI (2021) Effect of processing techniques and residual solvent on the thermal/mechanical properties of epoxy-cellulose nanocrystal nanocomposites. *Polym Eng Sci* 61:1281–1294
- Razavi R, Zare Y, Rhee KY (2017) A two-step model for the tunneling conductivity of polymer carbon nanotube nanocomposites assuming the conduction of interphase regions. *RSC Adv* 7:50225–50233
- Reid MS, Stimpson TC, Niinivaara E, Villalobos M, Cranston ED (2018) Comparing soft semicrystalline polymer nanocomposites reinforced with cellulose nanocrystals and fumed silica. *Ind Eng Chem Res* 57:220–230
- Rivera-Briso AL, Aachmann FL, Moreno-Manzano V, Serano-Aroca Á (2020) Graphene oxide nanosheets versus carbon nanofibers: enhancement of physical and biological properties of poly (3-hydroxybutyrate-co-3-hydroxyvalerate) films for biomedical applications. *Int J Biol Macromol* 143:1000–1008
- Saleh RI, Kim M, Baek SY, Cha C (2022) Chitosan-functionalized silica nanoparticles as a multifunctional coating material for improved water repellency, antimicrobial activity and mechanical strength of degradable bioplastics. *Cellulose* 29:7691–7701
- Shin H, Kim S, Kim J, Kong S, Lee Y, Lee JC (2022) Preparation of 3-pentadecylphenol-modified cellulose nanocrystal and its application as a filler to polypropylene nanocomposites having improved antibacterial and mechanical properties. *J Appl Polym Sci* 139:51848

- Takayanagi M, Uemura S, Minami S (1964) Application of equivalent model method to dynamic rheo-optical properties of crystalline polymer. *J Polym Sci Part C Polym Symposia* 5:113–122
- Tang J, Sisler J, Grishkewich N, Tam KC (2017) Functionalization of cellulose nanocrystals for advanced applications. *J Colloid Interface Sci* 494:397–409
- Wan C, Chen B (2012) Reinforcement and interphase of polymer/graphene oxide nanocomposites. *J Mater Chem* 22:3637–3646
- Wang B, Torres-Rendon JG, Yu J, Zhang Y, Walther A (2015) Aligned bioinspired cellulose nanocrystal-based nanocomposites with synergetic mechanical properties and improved hygro-mechanical performance. *ACS Appl Mater Interfaces* 7:4595–4607
- Xie X-L, Liu Q-X, Li RK-Y, Zhou X-P, Zhang Q-X, Yu Z-Z, Mai Y-W (2004) Rheological and mechanical properties of PVC/CaCO<sub>3</sub> nanocomposites prepared by in situ polymerization. *Polymer* 45:6665–6673
- Yang Y, He Q, Rao YN, Dai HL (2020) Estimation of dynamic thermo viscoelastic moduli of short fiber-reinforced polymers based on a micromechanical model considering interphases/interfaces conditions. *Polym Compos* 41:788–803
- Zappalorto M, Salviato M, Quaresimin M (2011) Influence of the interphase zone on the nanoparticle debonding stress. *Compos Sci Technol* 72:49–55
- Zare Y (2016) Modeling the strength and thickness of the interphase in polymer nanocomposite reinforced with spherical nanoparticles by a coupling methodology. *J Colloid Interface Sci* 465:342–346
- Zare Y, Rhee KY (2017) Dependence of Z parameter for tensile strength of multi-layered interphase in polymer nanocomposites to material and interphase properties. *Nanoscale Res Lett* 12:42
- Zare Y, Rhee KY (2017) A simple methodology to predict the tunneling conductivity of polymer/CNT nanocomposites by the roles of tunneling distance, interphase and CNT waviness. *RSC Adv* 7:34912–34921
- Zare Y, Rhee KY (2018) A multistep methodology for calculation of the tensile modulus in polymer/carbon nanotube nanocomposites above the percolation threshold based on the modified rule of mixtures. *RSC Adv* 8:30986–30993
- Zare Y, Rhee KY (2020) Significances of interphase conductivity and tunneling resistance on the conductivity of carbon nanotubes nanocomposites. *Polym Compos* 41:748–756
- Zare Y, Rhee KY (2022) Development of a model for modulus of polymer halloysite nanotube nanocomposites by the interphase zones around dispersed and networked nanotubes. *Sci Rep* 12:5406
- Zare Y, Rhee KY (2022) Effect of contact resistance on the electrical conductivity of polymer graphene nanocomposites to optimize the biosensors detecting breast cancer cells. *Sci Rep* 5406:1–10
- Zare Y, Rhee KY (2022) An innovative model for conductivity of graphene-based system by networked nano-sheets, interphase and tunneling zone. *Sci Rep* 12:1–9
- Zare Y, Rhee KY (2022) Minimum halloysite length for efficient load transfer through the interphase of polymer nanocomposites in biomedical applications. *JOM* 75:669–678
- Zare Y, Rhee KY (2023) Simulation of tensile strength for halloysite nanotube-filled system. *JOM* 75:592–602
- Zare Y, Rhee KY, Park S-J (2022) Two-stage modeling of tensile strength for a carbon-nanotube-based system applicable in the biomedical field. *JOM* 74:3059–3068
- Zhou J, Wang X, Liu X, Li X (2022) Design and synthesis of waterborne light-responsive cellulose nanocrystal/fluorinated polyacrylate films toward oil/water repellent and self-healing properties. *Cellulose* 29:7703–7720

**Publisher's Note** Springer Nature remains neutral with regard to jurisdictional claims in published maps and institutional affiliations.

Springer Nature or its licensor (e.g. a society or other partner) holds exclusive rights to this article under a publishing agreement with the author(s) or other rightsholder(s); author self-archiving of the accepted manuscript version of this article is solely governed by the terms of such publishing agreement and applicable law.